Effect of Alloying Elements on Crevice Corrosion Inhibition of Nickel-Chromium-Molybdenum-Tungsten Alloys under Aggressive Conditions: An Electrochemical Study

A.K. Mishra[1] and D.W.Shoesmith[*1,2]
[1]Department of Chemistry
Western University, London, ON, N6A 5B7, Canada

[2]Surface Science Western
999 Collip Circle, London, ON, N6G 0J3, Canada

The effects of Cr, Mo and W on the crevice corrosion of a number of commercial Ni-Cr-Mo (W) alloys in 1.0 mol/L NaCl were studied using the potentiodynamic-galvanostatic-potentiodynamic technique to measure film breakdown and repassivation potentials as well as protection temperatures. As expected, Cr is the key element determining resistance to crevice initiation but a substantial Mo alloy content is required to achieve maximum film stability especially at temperatures > 60°C. Molybdenum, not Cr, is the major element controlling crevice propagation and repassivation. If the protection temperature is accepted as the key indicator of overall alloy resistance then the resistance increases in the order; Alloy 625 < C-4 < C-276 < C-22 ~ Alloy 59 ~ C-2000 < Alloy 686. More generally, this order could be written; High Cr-Low Mo < Low Cr – High Mo < High Cr-High Mo < High Cr-High (Mo + W). The individual influences of Mo and W appear to be inseparable and, while adding W improved the resistance, adding the equivalent amount of Mo could achieve the same improvement.

Keywords: PD-GS-PD technique, Ni-Cr-Mo-W alloys, Crevice Corrosion, Repassivation Potential, Protection Temperature

* (Author for Correspondence) dwshoesm@uwo.ca

Introduction

Nickel-based metals, alloyed with Cr, Mo, W and other elements are widely used for equipment construction in the petrochemical, chemical process, and power industries because of their excellent corrosion resistance in both oxidizing and reducing environments. The presence of sufficient Cr enforces the growth of a passive barrier oxide layer of Cr_2O_3 on the surface, and Mo and W appear to retard the propagation of localized corrosion if the passive film is breached. Thus, optimization of the concentration of Cr, Mo and W is the key feature in developing Ni-Cr-Mo and Ni-Cr-Mo-W alloys which are resistant to uniform and localized corrosion and stress corrosion cracking [1, 2].

The passive film properties of a number of Ni-Cr-Mo (W) alloys were studied at different potentials and temperatures in acidic solutions by Lloyd et al. [3] using various electrochemical and surface characterization techniques. Both potentiostatic and potentiodynamic experiments showed that C-22 (UNS N06022) has a lower passive current density than C-276 (UNS N10276). This was attributed to the higher Cr content in C-22 which results in the growth of a more protective Cr/Ni oxide barrier layer at the alloy oxide interface. The effects of Cr, Mo and W on passive film properties and, to some extent, on localized corrosion were studied for the alloys C-4 (UNS N06455), C-276, 625 (UNS N06625), C-22 and C-2000 (UNS N06200) [4]. High Cr (> 20%, wt.%) containing alloys demonstrated better passive film properties than low Cr- containing alloys. While improved passivity was generally attributed to the alloy Cr content, Mo and W were found to segregate to the outer regions of the film, and, at high potentials when oxidation of Cr (III) to Cr (VI) initiates, were found to play an important role in suppressing the onset of transpassivity. As a consequence, Mo and W play a dominant role in the control/inhibition of localized corrosion in aggressive environments [4]. According to this study,

C-22 and C-2000, which contain high Cr and high Mo or Mo + W, provide better localized corrosion resistance in the aggressive environments than the other studied alloys (C-276 and C-4).

Jakupi et al. [5-9] used electrochemical and surface analytical techniques to determine the relationship between passive film impedance properties and composition in aggressive environments. The film properties on C-22 were investigated at different potentials in concentrated chloride (5 mol/L) solution using electrochemical impedance spectroscopy (EIS) and X-ray photoelectron spectroscopy (XPS). A direct relationship between film resistance and the Cr (III) oxide content of the barrier layer oxide film was observed [5]. A more extensive XPS study [10] subsequently confirmed this relationship and also showed that at more positive potentials when the Cr (III) content decreased, due to its oxidation to the more soluble Cr (VI), the Mo (VI) and W (VI) contents in the film increased substantially. Time of flight secondary ion mass spectrometry (ToF-SIMS) analyses on C-22 and on C-2000 showed the VI oxidation states of Mo and W accumulated at the oxide/solution interface, consistent with the previous observations in acidic solutions [3,4] although the extent of segregation to the outer surface was not so dramatic.

To understand the effect of Cr and Mo on the inhibition of localized corrosion behavior, crevice corrosion studies on Alloy 625, C-276 and Alloy G-3 (UNS N06985) were performed by Lillard et al. [11] in expected critical crevice solutions (CCS). Potentiodynamic results showed that an increase in Mo content resulted in a lower passive current density and a smaller dissolution rate associated with the active region. A crevice corrosion resistance ranking (C-276 > Alloy 625 > Alloy G-3), based on an increase in Mo content from Alloy G-3 to C-276, was proposed. The study further suggested that Mo alloying controls the crevice propagation rate.

Kehler and Scully [12] studied the crevice corrosion susceptibility of Alloy 625 and C-22 in an acidic solution. The metastable corrosion event rate, recorded from current-time transients, was found to increase with an increase in applied potential and temperature and the increase was more significant for Alloy 625 compared to C-22. Also, the depth of penetration due to crevice corrosion was higher for Alloy 625 than C-22. Since, both alloys have a similar Cr content, therefore, the differences in the crevice corrosion behavior was attributed to their Mo (or Mo + W) content, i.e., a higher Mo (or Mo + W) content in C-22 results in better crevice corrosion resistance.

Wong and Buchheit [13] studied the effect of Cr and Mo on the localized corrosion behavior in Ni-Cr-Mo alloys. It was observed that there was a reduction in the number of metastable pitting events with an increase in the Cr and Mo concentrations. An increase in Mo concentration resulted in a lower peak pitting current and a decrease in the rate of the fastest growing pits. Since, metastable pits are precursors to stable pits [14], this reduction in the number and size of metastable pit events led to an improvement in the alloy's resistance to localized corrosion.

The effect of Mo and W on galvanostatically-driven crevice propagation was also studied on the C-22 and C-2000 alloys [6]. Scanning electron microscopy (SEM) images and energy dispersive X-ray (EDX) mapping shows an accumulation of insoluble corrosion product, enriched with Mo, O and Mo, W, O at propagating sites for C-2000 and C-22, respectively, in agreement with the results reported by other researchers [15]. Raman spectroscopy results [6] indicated that the insoluble products formed at active locations within the crevice were polymeric Mo species (including W in the case of C-22) which control the crevice propagation rate and whose accumulation inhibits the depth of corrosion penetration [7]. These results are consistent

with those of Hayes et al. [16] who also claimed that, while Cr had the dominant influence on passivity, Mo was responsible for controlling pit propagation and promoting repassivation.

The corrosion behavior of C-22, C-22HS (UNS N07022) and Hybrid-BC1 alloy (UNS N10362) in 1M HCl solution at 90^0C was recently studied by Zadorozne et al. [17]. The corrosion rate, calculated from the Stern-Geary equation, shows that the anodic dissolution in the active potential range was mainly controlled by the Mo content, the higher Mo content of the Hybrid-BC1 alloy resulting in better corrosion resistance in the active region compared to C-22 and C-22HS. On the contrary, the Hybrid-BC1 alloy showed a higher passive current density (obtained from potentiodynamic polarization graphs) compared to C-22 and C-22HS. This poorer passivity of the Hybrid-BC1 alloy is a result of a lower Cr content. Crevice repassivation potentials ($E_{R,CREV}$) were obtained by the potentiodynamic-galvanostatic-potentiodynamic (PD-GS-PD) technique [18], using a multiple crevice assembly (MCA) arrangement, for C-22, C-22HS and Hybrid-BC1 in chloride solution at 90^0C. A significantly higher $E_{R,CREV}$ was obtained for the Hybrid-BC1 alloy compared to C-22 and C-22HS, which suggests that the higher Mo content in Hybrid-BC1 alloy aids in repassivation too.

In this study, a systematic investigation of the susceptibility to crevice corrosion initiation and the early stages of propagation has been undertaken for a range of commercially-available Ni-Cr-Mo (W) alloys. In addition, attention has been paid to the synergistic effect of one alloying element on another by comparing the behavior of alloys which differ in only one alloying component, with the primary emphasis on the understanding of the effects of Cr, Mo, and W.

The alloys studied were C-4, C-276, Alloy 625, C-22, C-2000, Alloy 59 (UNS N06059)

and Alloy 686 (UNS N06686). The comparison of alloys is based on breakdown potential (E_b), crevice repassivation potential ($E_{R,CREV}$) and protection temperature (T_{PROT}) measurements made using the PD-GS-PD technique. This technique allows very reproducible measurements. A detailed description of this technique has been reported elsewhere [18] and it has been successfully applied to a range of different corrosion resistant alloys in various solutions [17-22]. Experiments were conducted using both the MCA [17-23] and a single crevice arrangement [5-9].

Experimental

Materials and Solutions

The compositions of the alloys are listed in Table 1. The C-4, C-276, Alloy 625, C-22 and C-2000 alloys were supplied by Haynes International (USA), Alloy 59 by ThyssenKrupp (USA) and Alloy 686 by Special Metals (USA). Experiments were conducted in continuously deaerated 1M NaCl solution at various temperatures. Solutions were prepared using de-ionized (DI) Milli-Q Millipore water (18.2 MΩ cm) and reagent grade salts. A fresh solution was prepared for each experiment and all experiments were repeated at least twice to confirm reproducibility.

Electrode Preparation and Electrochemical Techniques

Multiple Crevice Assemblies

Cubic specimens with a total surface area of 14 cm^2 were cut from the plate materials. A small tapped hole was machined in the top of the specimen to enable contact, via a cylindrical rod, to external circuitry. This rod was sheathed in glass and sealed with a teflon gasket to prevent contact with the electrolyte. A 7.0 mm diameter hole was machined in the center of the

cubic specimen which was then polished with a series of wet silicon carbide papers up to 1200 grit, rinsed with deionized water and acetone, and then air dried prior to an electrochemical experiment. A teflon-wrapped ceramic crevice former, tightened to a torque of 70 in-lb by Ti bolts, was used to create 12 crevices. A platinum foil and a saturated calomel electrode (SCE) were used as the counter and reference electrodes, respectively.

A standard jacketed, three-electrode cell was connected to a water circulating thermostatic bath allowing control of the solution temperature to within 1°C. The reference and counter electrodes were housed in separate compartments attached to the main body of the glass cell through glass frits. The cell was placed in a Faraday cage to reduce external sources of electrical noise. Crevice corrosion experiments were performed using the PD-GS-PD technique [18] to measure the characteristic potentials (E_b and $E_{R,CREV}$) and temperature (T_{PROT}).

Potentiodynamic scans were performed at a scan rate of 0.167 mV/s from a potential 150-250mV below E_{CORR} to a potential above the breakdown potential (E_b) until a current of 30 μA was reached. This current was then maintained galvanostatically for 40 hours. Finally the potential was scanned back to a lower potential at a rate of 0.167 mV/s. Galvanostatic control was maintained for 40 hours, rather than the normal 2 hours [18], to ensure the establishment of active propagation conditions.

Single Crevice Assembly

Single crevice experiments were conducted inside a pressure vessel which allows boiling to be suppressed at T > 100°C. The vessel was lined with a 3mm thick cylindrical PTFE liner to avoid direct solution contact with the titanium pressure vessel wall. The creviced (working) electrode was suspended from a thin cylindrical rod of the same material enclosed in heat-shrink

PTFE tubing to avoid electrical contact with the pressure vessel. The counter electrode was made from the same material as the working electrode. A homemade Ag/AgCl (saturated KCl) reference electrode was used [24]. The potential of this electrode (-45mV vs SCE) was checked against a commercial saturated calomel electrode (SCE), used only as a standard, before and after each experiment.

A schematic of the crevice electrode arrangement inside the pressure vessel has been reported elsewhere [5-9]. The geometry of the working electrode was designed to avoid unwanted crevices. The crevice former was a PTFE slice fixed between the flat metal surface and a polysulfone coupon. In this study the crevice design was modified slightly with the crevice former surface area made smaller than the flat surface area of metal in order to better define the crevice mouth and to confine any propagation to the flat surface of the specimen. The creviced assembly was held together with insulated threaded bolts and metal nuts to ensure that the defined working electrode surface would be the only creviced metal area exposed to solution. The creviced face of the working electrode was polished using the same procedure employed with the MCA.

To prevent boiling of the electrolyte solution, the pressure vessel was pressurized with 0.4 MPa of Ar gas. On first exposure to the solution, the electrode was allowed to stabilize on open circuit for 8 hours. Subsequently, crevice corrosion was initiated galvanostatically (5 µA or 20 µA) and the current maintained throughout the 48 hours of the experiment.

Results and Discussion

Effect of Cr on Crevice Corrosion

To study the effect of Cr, the Alloys C-276 and 686 were compared, since both have

similar Mo and W contents and differ only significantly in their Cr content (16 wt% for C-276 compared to 21 wt% for 686). The small difference in Fe content (Table 1) is not expected to significantly affect the corrosion resistance, the primary purpose of its incorporation in Ni-based alloys being cost reduction [1].

Potentials recorded during the galvanostatic stage (the GS step in the PD-GS-PD measurement) are shown in Figure 1. The temperatures at which active crevice conditions were established on the two alloys are identified by the significant drop in potential at 40^0C to 45^0C for C-276 alloy and 75^0C to 80^0C for Alloy 686. From these plots, the T_{PROT} values of ~ 40^oC for C-276 and ~ 75^oC for Alloy 686 were established.

Figure 2 shows the E_b and $E_{R,CREV}$ values as a function of temperature for both these alloys. A significant increase in E_b, especially at higher temperature, was observed as a result of the increased Cr content in Alloy 686 compared to C-276. These results are consistent with those of other investigators [4] who proposed that higher Cr content results in a less defective, highly enriched Cr_2O_3 barrier layer. However, once crevice corrosion initiated on both alloys (for $T > T_{PROT}$), the similarity in $E_{R,CREV}$ values indicated no significant effect of Cr on crevice repassivation.

To understand the effect of Cr in more detail, two more Ni-Cr-Mo alloys (C-4 and Alloy 59) were studied. Unlike, C-276 and 686, C-4 and 59 contain no W (Table 1). Both C-4 and 59 have similar Mo but differ in Cr content, with C-4 having 7% (wt.%) less than 59. Unsurprisingly, Alloy 59 had a higher E_b than C-4 and, consistent with the results for Alloy 686 and C-276, both alloys exhibited a similar $E_{R,CREV}$, Figures 3 and 4. Furthermore, C-4 containing relatively low Cr and low Mo initiated crevice corrosion at a temperature as low as 35^0C (Figure

3a). Based on these results on four different commercially-available Ni-Cr-Mo (W) alloys, it can be concluded that increasing the Cr content resulted in improved passivity and, thus, a higher E_b. However, Cr appeared to play little to no role in the control of crevice propagation and repassivation.

Effect of Mo on Crevice Corrosion

C-22 and Alloy 686 were selected to study the effect of Mo on crevice corrosion, since both alloys have similar Cr and W contents while C-22 has a 3% (wt.%) lower Mo content than Alloy 686 (Table 1). Figures 5 and 6 show the potentials (recorded during the galvanostatic period) and the variation of E_b and $E_{R,CREV}$ with temperature, respectively. The T_{PROT} for Alloy 686 was ~ 20°C higher than that for C-22 indicating that the high Mo (or Mo + W) content retarded the initiation of crevice corrosion as the temperature was increased. Comparison of the E_b values shows the higher Cr alloy (Alloy 686) exhibited slightly higher values (~ 50 mV at low temperatures decreasing to ~ 20 mV at higher temperatures) than C-22 except at the highest temperature when the difference widened to ~ 160 mV. This minor difference in E_b values suggests the small difference in Mo content did not influence the passivity significantly. These results confirm the importance of Cr in preventing film breakdown, any additional influence on passivity of Mo being minor except at the highest temperature (85°C, Figure 6). Given the similarities in E_b values for the two alloys, the initiation of crevice corrosion on C-22, but not Alloy 686, at lower temperatures suggested a role of Mo in preventing crevice initiation, especially with increasing temperature.

Since the influences of Cr and Mo (or Mo + W) are hard to separate, the behaviors of C-22 and Alloy 686 were compared at the higher temperature of 105°C using a single crevice

arrangement (Figure 7). In these experiments the potential of each alloy was followed for 48 hours at an applied current of either 5 µA or 20 µA. At the lower current (Figure 7a), after a single major event at ~ 16 hours, the potential on C-22 became unstable after ~ 28 hours. This behavior indicated continuous unsuccessful attempts to establish stable active crevice corrosion sites. By comparison, Alloy 686 established a stable potential at this current with only very minor, effectively negligible, negative-going transients. This is a strong indication that the increased Mo (Mo + W) content was suppressing the metastable activation events which eventually could lead to the establishment of active crevice corrosion sites. This is in consensus with the results reported by other researchers [12, 13].

To confirm this influence the experiment was repeated at a higher applied current when initiation would be expected to occur more readily. As shown in Figure 7b, this was the case, the initiation of stable crevice corrosion occurring on C-22 in 6 to 7 hours. By comparison active corrosion conditions were not established on the 686 alloy until > 27 hours even though the higher density of metastable events (compared to the density observed at 5 µA) suggested many attempted initiations occurred. The resistance to initiation on Alloy 686 is clearly indicated by the considerably higher potential required (at this higher current) before initiation finally occurs.

To investigate the importance of Mo in inhibiting crevice initiation, the crevice corrosion behavior of Alloy 625 and Alloy 59 were compared using the MCA arrangement, Figures 8 and 9. While both these alloys have a high (21 to 23 wt.%) Cr content, the Mo content of Alloy 625 (9 wt.%) is considerably lower than that of Alloy 59 (16 wt.%). Figure 9 shows little difference in E_b between the two alloys, at least for temperatures below 60°C, both being very positive, as expected for high Cr content alloys. However, once E_b was exceeded crevice corrosion initiated

on the low Mo-containing Alloy 625 at a temperature of 30°C compared to 60°C for the high Mo-containing Alloy 59 (Figure 8). At temperatures above 60°C, the influence of Mo on maintaining passivity was very marked. For Alloy 59 (16 wt% Mo), E_b decreased only marginally over the temperature range 60°C to 85°C while that for Alloy 625 (9 wt% Mo) fell substantially. The difference in E_b values at 85°C reached ~ 300 mV (Figure 9).

These results indicate a number of influences of Mo. In high Cr-high Mo (Mo + W) alloys, passivity appeared to be optimized but even a relatively small increase in Mo (Mo + W) inhibited crevice initiation even at temperatures as high as 105°C. As proposed previously by Kehler and Scully [12] and Wong and Buchheit [13], this appeared to be due to the ability of Mo to suppress the transition of metastable film breakdown events to stable active crevice sites.

However, experiments which compare alloys with high-Cr but significantly different Mo contents showed that initiation of active sites was not suppressed at lower Mo contents. Additionally, while a high Cr content may have led to high E_b values in low Mo alloys at low temperatures (< 60°C) the resistance to film breakdown at higher temperatures could not be maintained, E_b decreasing markedly with temperature for low Mo alloys. Although alloys with only a limited variation in Mo content were included in this study, a minimum Mo content > 9 wt% was required to achieve the high temperature resistance.

Effect of W on Crevice Corrosion

The alloy comparisons described so far could not separate the influences of Mo and W. In an attempt to distinguish these influences the behavior of Alloy 59 and Alloy 686 were compared. Both alloys have similar Cr and Mo contents but only Alloy 686 contains W (4 wt%). The characteristic potentials for these two alloys are shown in Figures 10 and 11. Both alloys

exhibited very high E_b values which were maintained up to 85°C, as expected for high Cr-high Mo alloys. However, T_{PROT} for Alloy 686 was ~ 20°C higher than the value for the W-free Alloy 59. While this clearly indicated a beneficial effect of W in preventing initiation it is feasible that a 4% increase in the Mo content rather than the addition of W could have achieved the same effect. Like Mo, W has been shown to form a protective oxide gel within active sites which inhibits crevice propagation and assists repassivation [6]. However, no individual separate influence of W was demonstrated.

Comparison of E_b, $E_{R,CREV}$ and T_{PROT} Values

The effect of alloying elements on E_b is summarized in Figure 12. The value of E_b can be taken as a measure of the passive oxide film resistance to breakdown: the higher the value the more stable the film. Two distinct categories can be distinguished: (1) alloys which have both a high Cr and high Mo (Mo + W) content (C-22, C-2000, Alloy 59 and Alloy 686) which exhibited high E_b values (within the shaded area in Figure 12); and (2), alloys with either a high Cr or high Mo (Mo + W) content (Alloy 625, C-4 and C-276), but not both, which had significantly lower E_b values.

Within this second group the alloy with the lowest E_b value was C-4 with a low Cr content. By comparison, Alloy 625, with a considerably higher Cr content, exhibited E_b values approaching those measured on the alloys in category (1) except at higher temperatures. While this difference between C-4 and Alloy 625 confirms the importance of Cr content in maintaining passivity, it is noteworthy that a similar improvement in E_b could be achieved for a low Cr alloy (C-276) by adding 4 wt% W, and this improvement is extended to higher temperatures. Within category 1 the differences were minor but Alloy 686 with high Cr and high (Mo + W) had the highest E_b values.

Figure 13 shows the plot of $E_{R,CREV}$ as a function of temperature for various Ni-Cr-Mo (W) alloys. This comparison yields similar trends with Cr, Mo and Mo + W content to that observed for E_b, but with some differences for the poorer performing alloys. When comparing E_b values (above) the poorest performing alloy (lowest E_b values), except at the highest temperatures, was the low Cr-high Mo C-4. By contrast, when comparing $E_{R,CREV}$ values, it is the high Cr-low Mo Alloy 625 which had the lowest values over the whole temperature range indicating that Mo, rather than Cr, is the key alloying component controlling propagation and assisting repassivation.

Consideration of the whole set of $E_{R,CREV}$ values shows that generally over the whole temperature range (up to 85°C) the order of increasing $E_{R,CREV}$ values, indicating a suppression of propagation and improved tendency to repassivate, was

High Cr-Low Mo < Low Cr-High Mo < High Cr-High Mo < High Cr-High Mo+W

When comparing all the alloys perhaps the most instructive parameter which yields an overall evaluation of resistance to crevice corrosion for a series of alloys is T_{PROT}, the temperature below which crevice corrosion does not initiate. These values, taken to be 5°C below the lowest temperature at which crevice initiation was observed, and hence a value of T_{PROT} obtained (Figure 13), are plotted in Figure 14 as a function of the Mo + W content of the alloy. It should be noted that the T_{PROT} for Alloy 625 is assumed to be around 25°C, since crevice corrosion was observed at the first temperature tested which was 30°C.

The two diagonal lines in Figure 14 show that two distinct classes of alloy can be defined; low-Cr and high-Cr. In both cases increasing the Mo + W content lead to an increase in the temperature range (25°C to T_{PROT}) over which the alloy was protected against crevice

corrosion. The synergistic effect of Cr and Mo (+W) was clearly demonstrated by the significantly better performance of the high-Cr alloys.

A common way to compare the localized performance of alloys is to calculate the pitting resistance equivalent number (PREN) [26]. Previous investigators [17] have used the relationship

$$PREN = \%Cr + 3.3\%(Mo + 0.5W) \quad (1)$$

to calculate the influence of alloy composition on resistance to localized corrosion. The applicability of this relationship can be deduced by plotting PREN as a function of T_{PROT}, Figure 15. Note, no value for Alloy 625 is included since no reliable T_{PROT} value was actually recorded for this alloy (as noted above). While a reasonable relationship is observed for 5 of the alloys, the crevice corrosion resistance of the C-22 alloy is significantly underestimated by this relationship.

A possibility is that the influence of W on the behavior of C-22 is underestimated. Consequently, the second line in Figure 14 shows the T_{PROT} values plotted against a PREN value calculated assuming the effect of W is identical to that of Mo; i.e.,

$$PREN = \%Cr + 3.3\% (Mo + W) \quad (2)$$

This adjustment does not lead to a better relationship, the PREN value for C-276 being uncorrelated to the other values. While it is feasible that an improvement of the fit to a straight line could be achieved by varying the relative importance of the individual elements in the calculation, the empirical nature of the parameter, PREN, and the absence of any demonstrated mechanistic connection to T_{PROT} makes this a somewhat artificial exercise. That both lines are equally limited in their ability to define the relative contributions of Mo and W may reflect the similar chemical behavior of these two elements in controlling crevice propagation [6]. These

relationships are best used only as qualitative indicators of the function of these two elements in determining the resistance to crevice corrosion.

Summary and Conclusions

The effects of the alloying elements Cr, Mo and W on the crevice corrosion of commercial Ni-Cr-Mo(W) alloys in 1.0 mol/L NaCl solution have been studied using the PD-GS-PD technique to measure film breakdown and alloy repassivation potentials and protection temperatures; i.e., the temperature below which crevice corrosion does not initiate. While the Cr content is the key alloying addition determining passive film stability, the presence of a substantial Mo content (>> 9 wt%) is required to achieve maximum film stability against breakdown under creviced conditions. This is particularly the case for temperatures > 60°C.

Mo is the key alloying element influencing repassivation after crevice propagation, the repassivation potential ($E_{R,CREV}$) showing a clear increase with increasing Mo (or Mo + W) content indicating a greater driving force for repassivation.

If the protection temperature (T_{PROT}) is accepted as a key indicator of an alloy's overall resistance to crevice corrosion then the alloys can be ranked in the following order of increasing resistance,

Alloy 625 < C-4 < C-276 < C-22 ~ Alloy 59 ~ C-2000 < Alloy 686

More generally this order could be written as

High Cr-Low Mo < Low Cr-High Mo < High Cr-High Mo < High Cr-High Mo+W

Attempts to separate the influences of Mo and W were not successful. While it was shown that adding W improved the resistance, it is possible that increasing the Mo content by a similar amount would have produced the same improvement.

Using values of PREN, calculated by either separating or combining the influences of Mo and W produced only qualitatively linear relationships but could not separate the influences of the two elements. While PREN values offer guidance in alloy design they should not be considered quantitative.

Acknowledgements

This research was funded by the Canadian Natural Sciences and Engineering Research Council (NSERC). The authors also acknowledge Haynes International, Thyssenkrupp and Special Metals for providing the samples.

References

[1] P. Crook, D. Klarstrom, ASM Handbook, Vol. 13B, Materials Park, OH: ASM International (2005): p. 228.

[2] W. Z. Friend, Corrosion of Nickel and Nickel-Based Alloys, New York, NY: John Wiley and Sons (1980): p. 292

[3] A. C. Lloyd, D. W. Shoesmith, N. S. McIntyre, J. J. Noel, *J. Electrochem. Soc.*, **150** (2003): p. B120

[4] A. C. Lloyd, J. J. Noel, S. McIntyre, D. W. Shoesmith, *Electrochim. Acta*, **49** (2004): p. 3015

[5] P. Jakupi, D. Zagidulin, J.J. Noel, D.W. Shoesmith, *Electrochim. Acta*, **56** (2011):p. 6251

[6] P. Jakupi, F. Wang, J.J. Noel, D.W. Shoesmith, *Corros. Sci.*, **53** (2011): p.1670

[7] P. Jakupi, J.J. Noel, D.W. Shoesmith, *Corros. Sci.*, **53** (2011): p. 3122

[8] P. Jakupi, J.J. Noel, D.W. Shoesmith, *Corros. Sci.*, **54** (2012): p. 260

[9] P. Jakupi, J.J. Noel, D.W. Shoesmith, *Electrochem. and Solid-State Letters*, **13** (2010): p. C1

[10] X. Zhang, D. Zagidulin, D.W. Shoesmith, *Electrochim. Acta*, **89** (2013): p. 814

[11] R. S. Lillard, M. P. Jurinski, J. R. Scully, *Corrosion*, **50** (1994): p. 251

[12] B. A. Kehler, J. R. Scully, *Corrosion*, **61** (2005): p. 665

[13] F. Wong, R. Buchheit, *ECS Trans.*, **16** (2009): p. 91

[14] G. S. Frankel, *J. Electrochem. Soc.*, **145** (1998): p. 2186

[15] X. Shan, J.H. Payer, *J. Electrochem. Soc.*, **156** (2009): p. C313

[16] J. R. Hayes, J. J. Gray, A. W. Szmodis, C. A. Orme, *Corrosion*, **62** (2006): p. 491

[17] N.S. Zadorozne, C.M. Giordano, M.A. Rodriguez, R.M. Carranza, R.B. Rebak, *Electrochim. Acta*, **76** (2012): p. 94

[18] A.K. Mishra, G.S. Frankel, *Corrosion,* **64** (2008): p. 836

[19] M.R. Ortiz, M.A. Rodriguez, R.M. Carranza, R.B. Rebak, *Corrosion*, **66** (2010): p. 1

[20] M. Miyagusuku, R.M. Carranza, R.B. Rebak, CORROSION/2011, paper no. 11202, (Houston, TX: NACE 2011)

[21] M.R. Ortiz, M.A. Rodriguez, R.M. Carranza, R.B. Rebak, *Corros. Sci.*, **68** (2013): p. 72

[22] C.M. Giordano, M.R. Ortiz, M.A. Rodriguez, R.M. Carranza, R.B. Rebak, *Corros. Engg., Sci. and Tech.*, **46** (2011): p. 129

[23] K.J. Evans, A. Yilmaz, S.D. Day, L.L. Wong, J.C. Estill, R.B. Rebak, *JOM*, **57** (2005): p. 56

[24] X. He, J.J. Noel, D.W. Shoesmith, *J. Electrochem. Soc.*, **149** (2002): p. B440

[25] Z. Szklarska-Smialowska, Pitting and Crevice Corrosion of Metals, Houston, TX: NACE International (2005)

List of Table

List of Figures

Figure 11. Eb and ER,CREV values recorded using the PD-GS-PD technique on MCA specimens of Alloy 59 and Alloy 686 at different temperatures in 1M NaCl solution

Figure 12. Eb values for various commercial Ni-Cr-Mo (W) alloys as a function of temperature measured in 1M NaCl solution

Figure 13. ER,CREV values for various commercial Ni-Cr-Mo (W) alloys as a function of temperature measured in 1M NaCl solution

Figure 14. TPROT values as a function of the Mo+W content of a series of commercial Ni-Cr-Mo (W) alloys measured in 1M NaCl solution

Figure 15. Relationship between TPROT (from Figure 14) and PREN values calculated for various Ni-Cr-Mo (W) alloys: (1) PREN values calculated using relationship (1); (2) PREN values calculated using relationship (2)

 http://dx.doi.org/10.5006/1170

Table 1. Nominal chemical compositions of the alloys studied (wt. % of major alloying element)

Alloying element	C-4 UNS N06455	C-276 UNS N10276	Alloy 625 UNS N06625	C-22 UNS N06022	Alloy 59 UNS N06059	C-2000 UNS N06200	Alloy 686 UNS N06686
Cr	16	16	21	22	23	23	21
Mo	16	16	9	13	16	16	16
W	-	4	-	3	-	-	4
Fe	3	5	5	3	1	1	1
Cu	-	-	-	-	-	1.6	
Ni	64	57	62	56	59	58	58

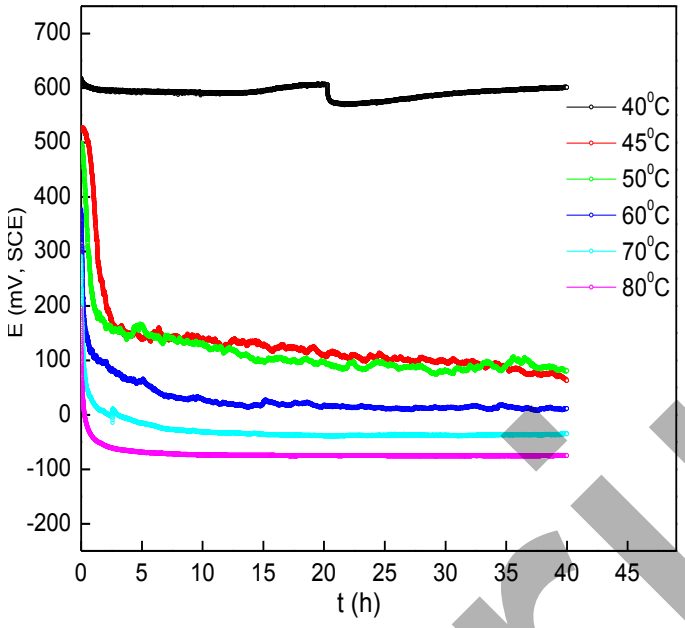

(a)

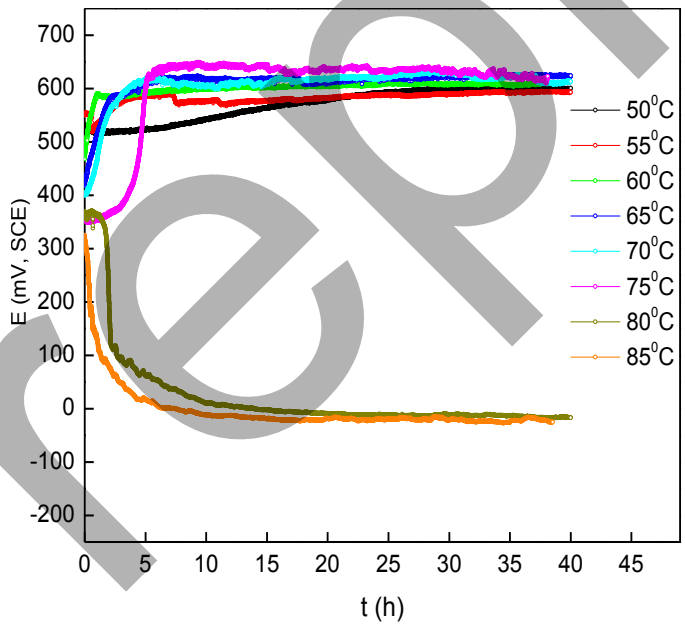

(b)

Figure 1. Potentials recorded on MCA specimens during the galvanostatic stage (GS) when using the PD-GS-PD technique: (a) C- 276 and (b) Alloy 686 at various temperatures in 1 M NaCl solution

http://dx.doi.org/10.5006/1170

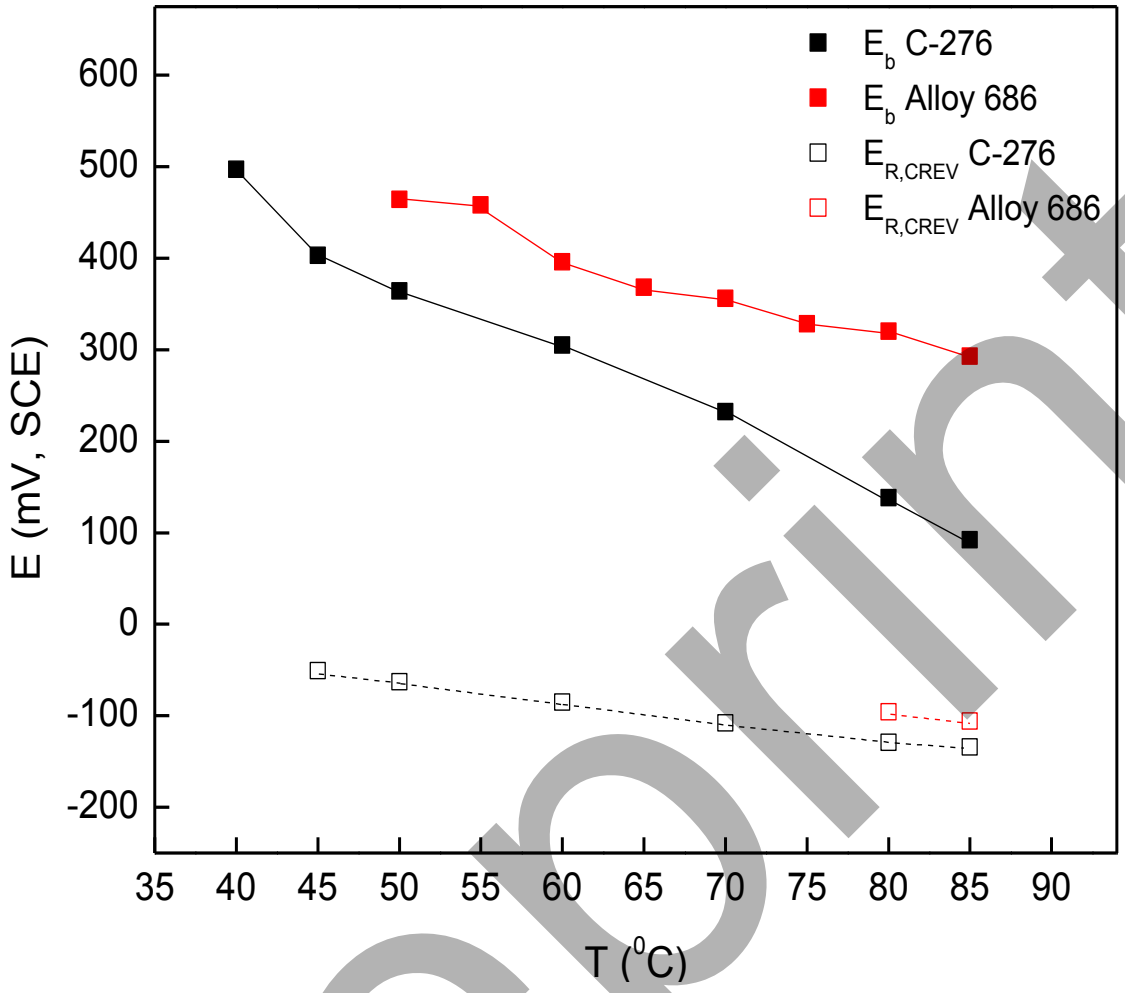

Figure 2. E_b and $E_{R,CREV}$ values recorded using the PD-GS-PD technique on MCA specimens of C-276 and alloy 686 at different temperatures in 1M NaCl solution

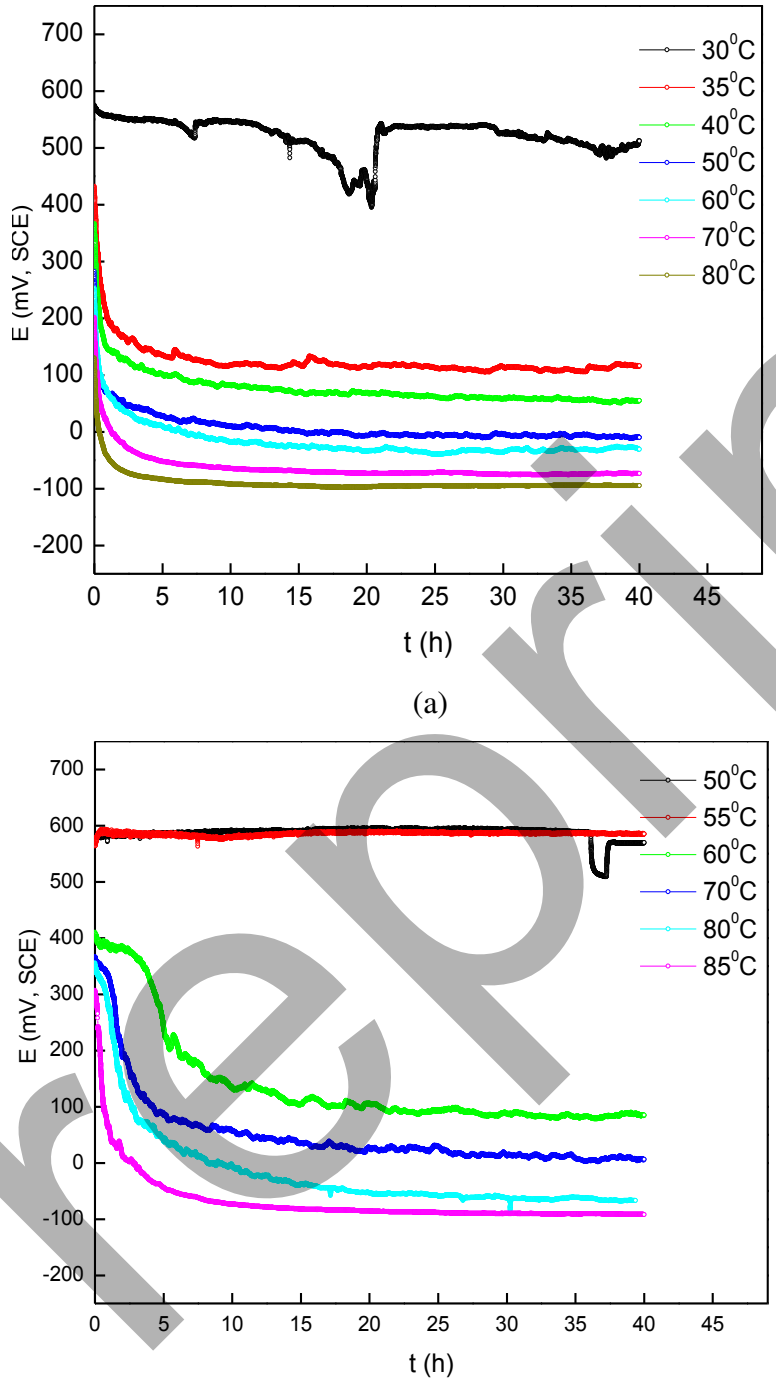

Figure 3. Potentials recorded on MCA specimens during the galvanostatic stage (GS) when using the PD-GS-PD technique: (a) C- 4 and (b) Alloy 59 at various temperatures in 1M NaCl solution

http://dx.doi.org/10.5006/1170

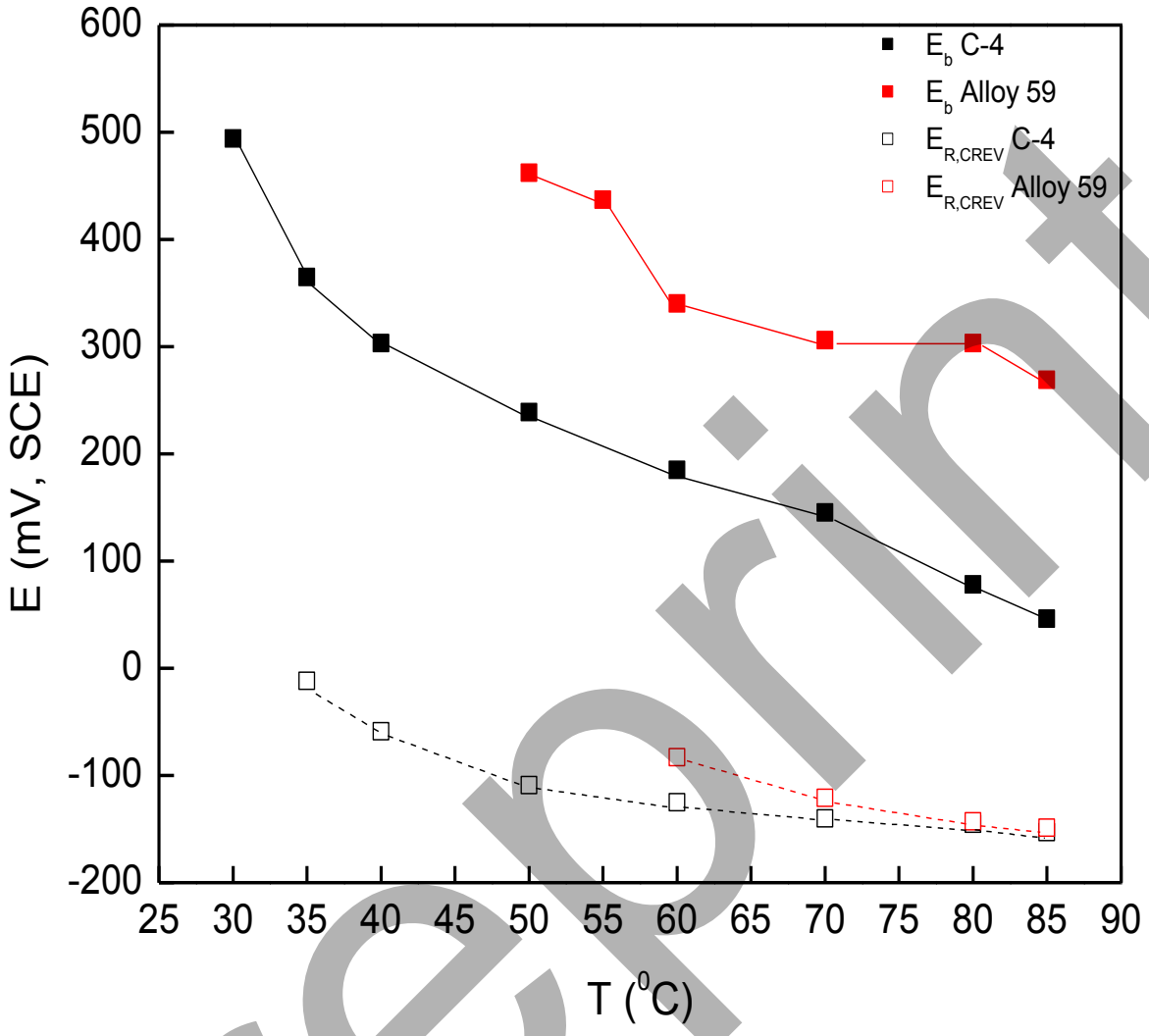

Figure 4. E_b and $E_{R,CREV}$ values recorded using the PD-GS-PD technique on MCA specimens of C-4 and Alloy 59 at different temperatures in 1M NaCl solution

http://dx.doi.org/10.5006/1170

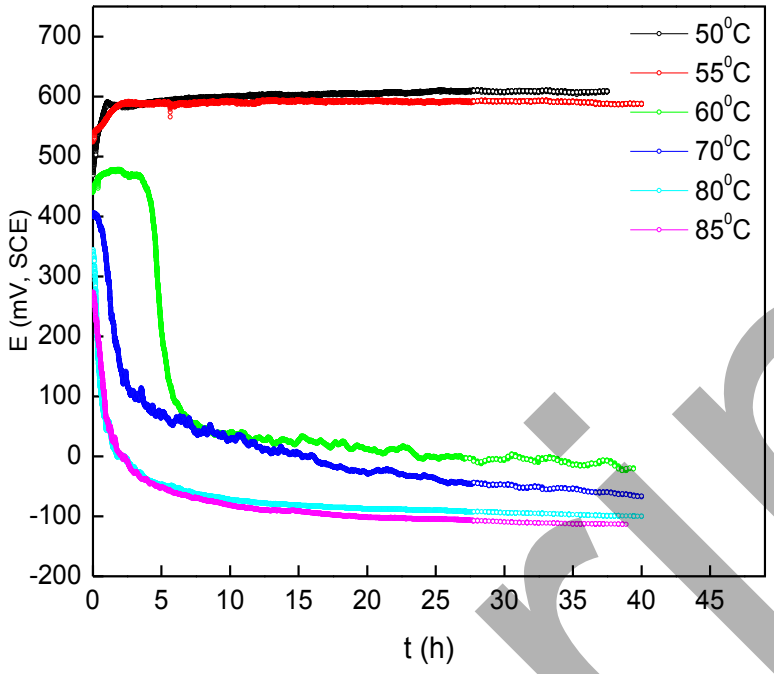

(a)

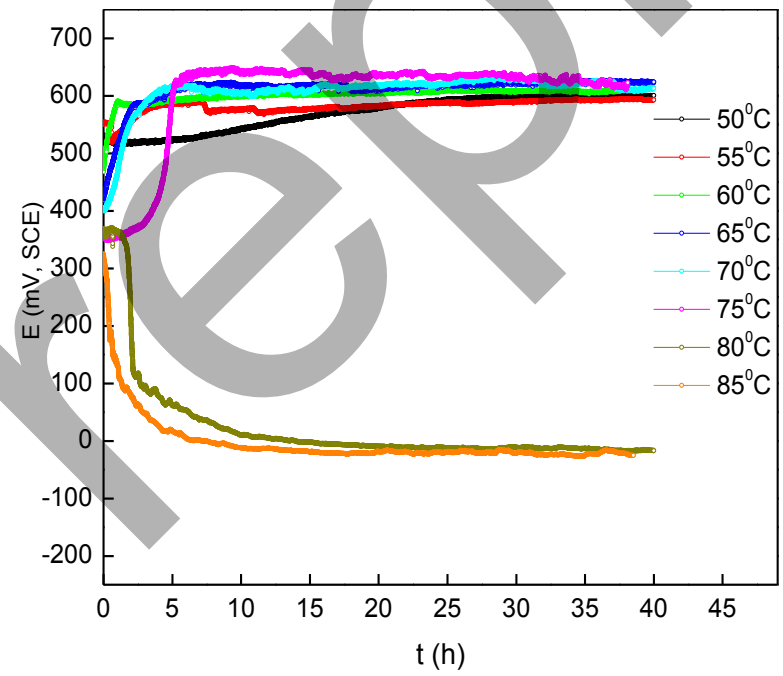

(b)

Figure 5. Potentials recorded on MCA specimens during the galvanostatic stage (GS) when using the PD-GS-PD technique: (a) C- 22 and (b) Alloy 686 at various temperatures in 1M NaCl solution

http://dx.doi.org/10.5006/1170

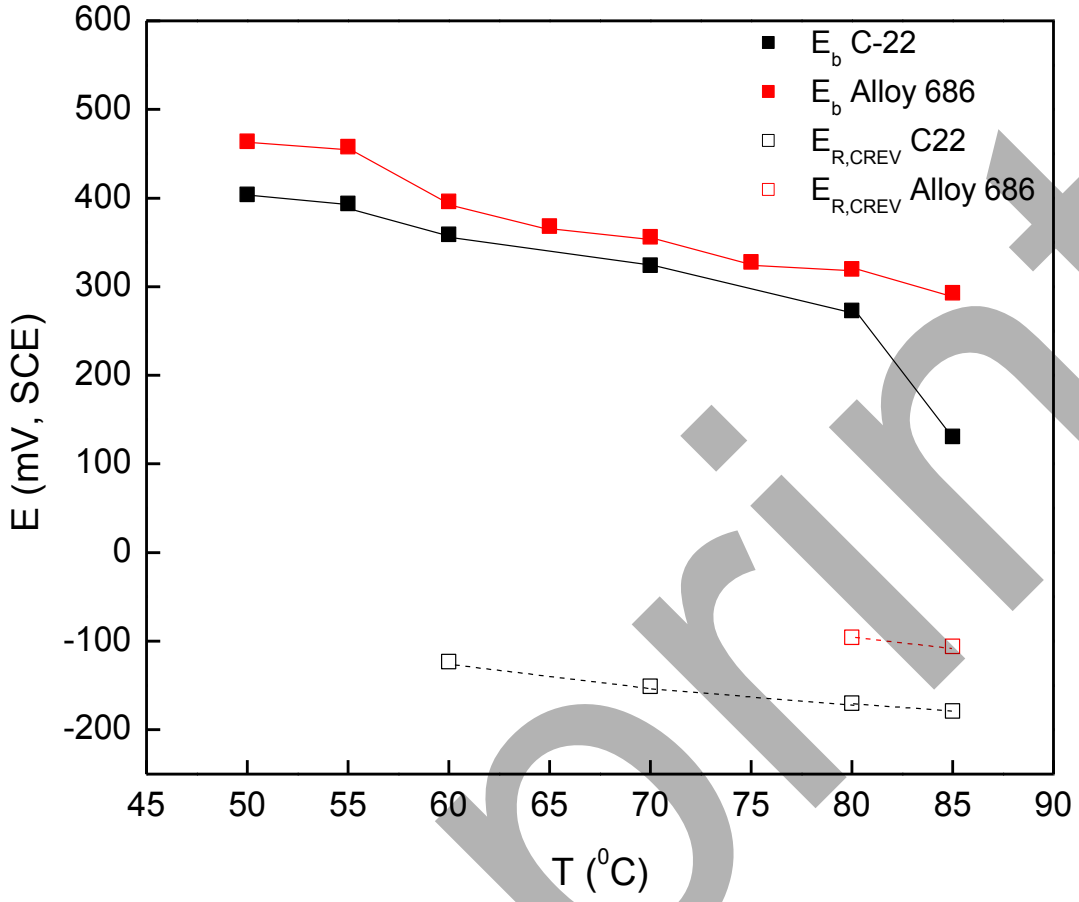

Figure 6. E_b and $E_{R,CREV}$ values recorded using the PD-GS-PD technique on MCA specimens of C-22 and Alloy 686 at different temperatures in 1M NaCl solution

http://dx.doi.org/10.5006/1170

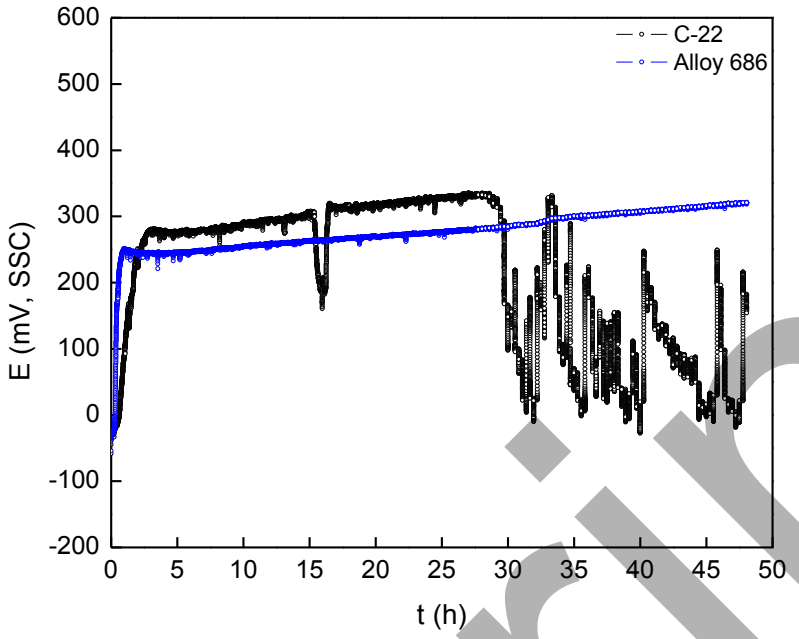

(a)

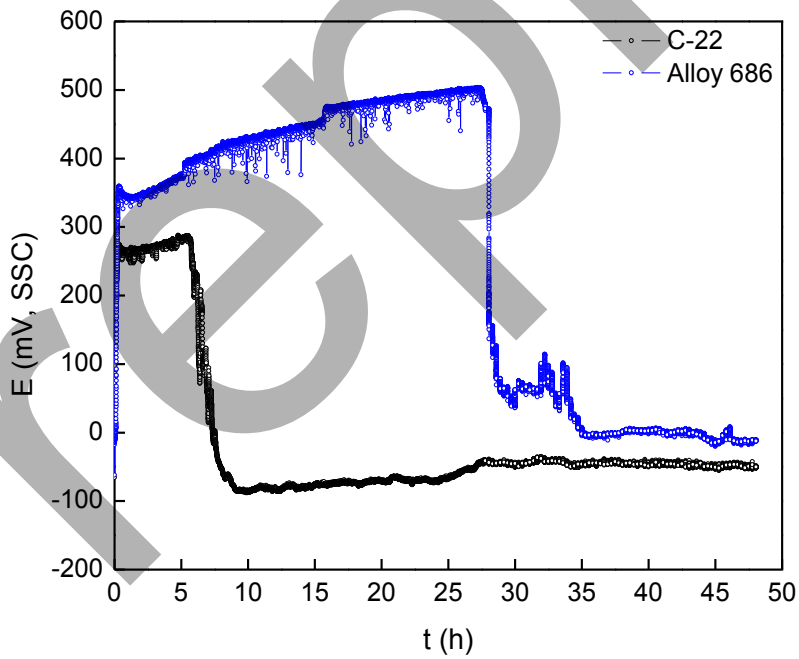

(b)

Figure 7. Potentials recorded on single crevice electrodes during galvanostatic experiments on C-22 and alloy 686 at 105^0C in 1M NaCl solution: (a) 5µA and (b) 20 µA

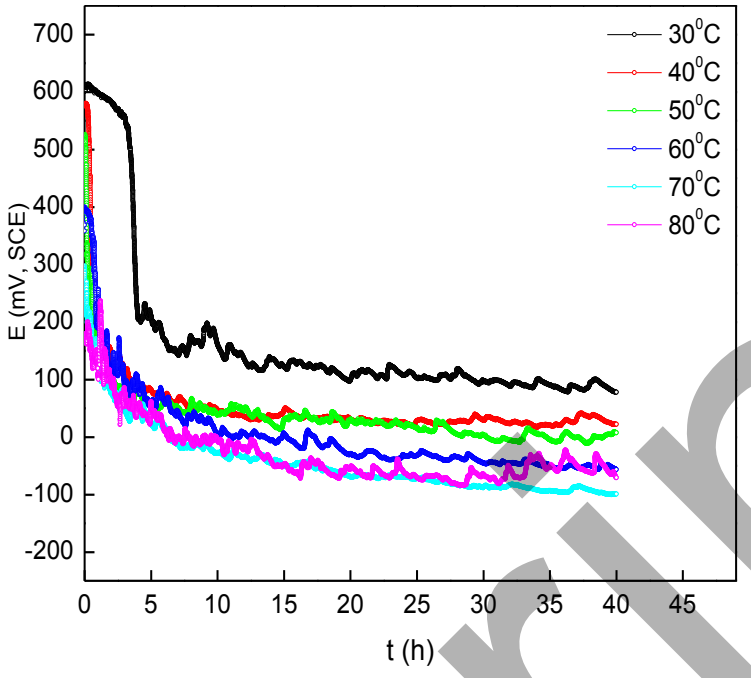

(a)

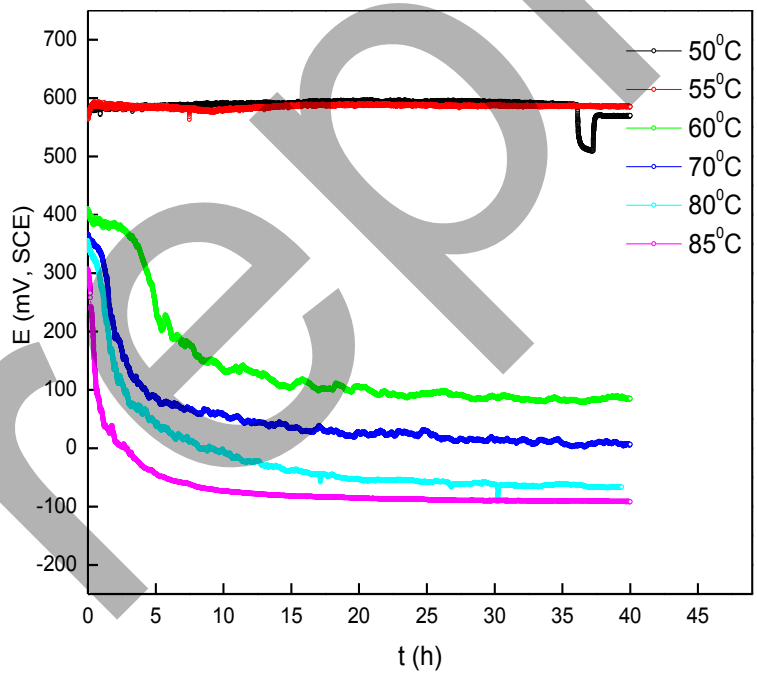

(b)

Figure 8. Potentials recorded on MCA specimens during the galvanostatic stage (GS) when using the PD-GS-PD technique: (a) Alloy 625 and (b) Alloy 59 at various temperatures in 1M NaCl solution

http://dx.doi.org/10.5006/1170

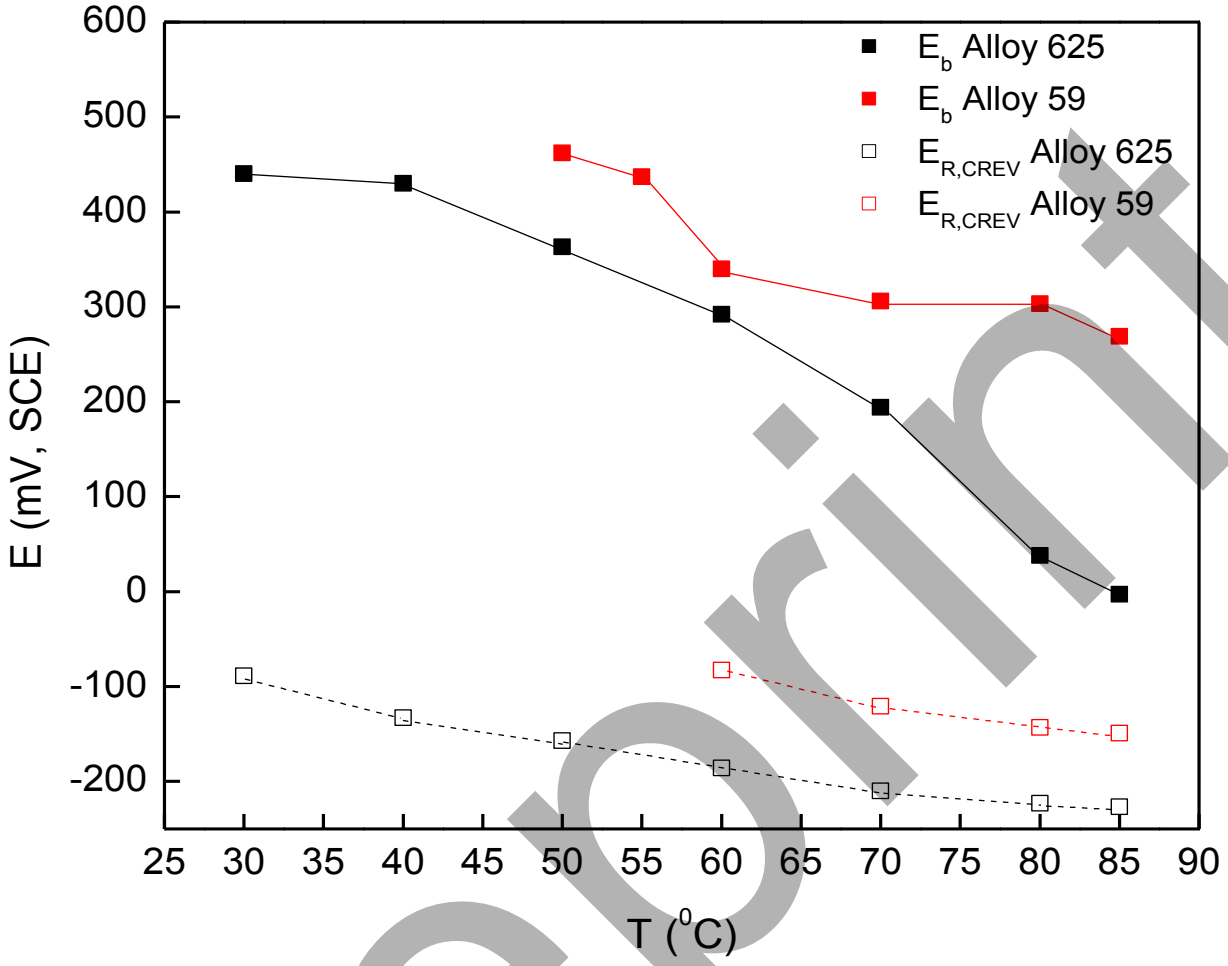

Figure 9. E_b and $E_{R,CREV}$ values recorded using the PD-GS-PD technique on MCA specimen of Alloy 625 and Alloy 59 at different temperatures in 1M NaCl solution

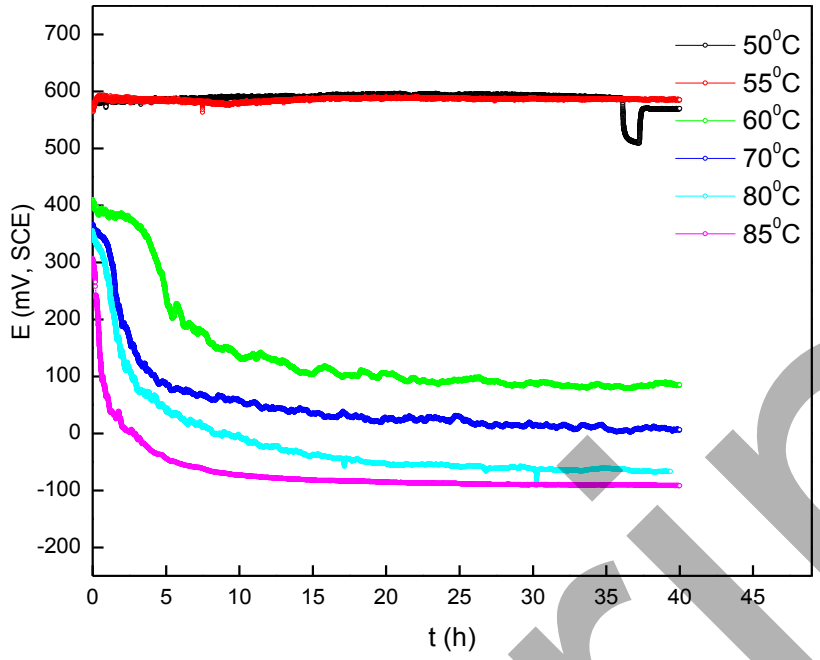

(a)

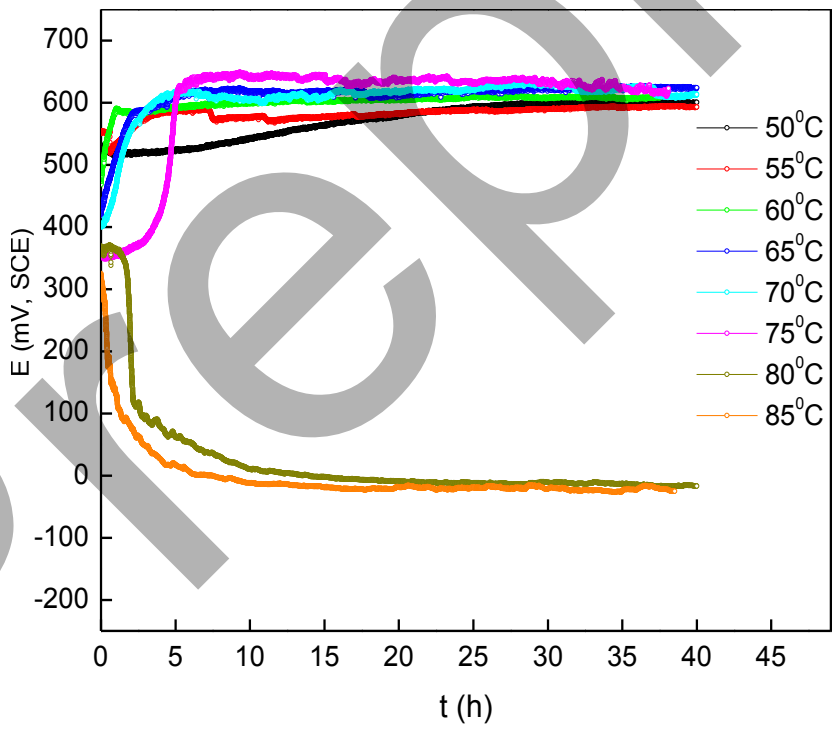

(b)

Figure 10. Potentials recorded on MCA specimens during the galvanostatic stage (GS) when using the PD-GS-PD technique: (a) Alloy 59 and (b) Alloy 686 at various temperatures in 1M NaCl solution

http://dx.doi.org/10.5006/1170

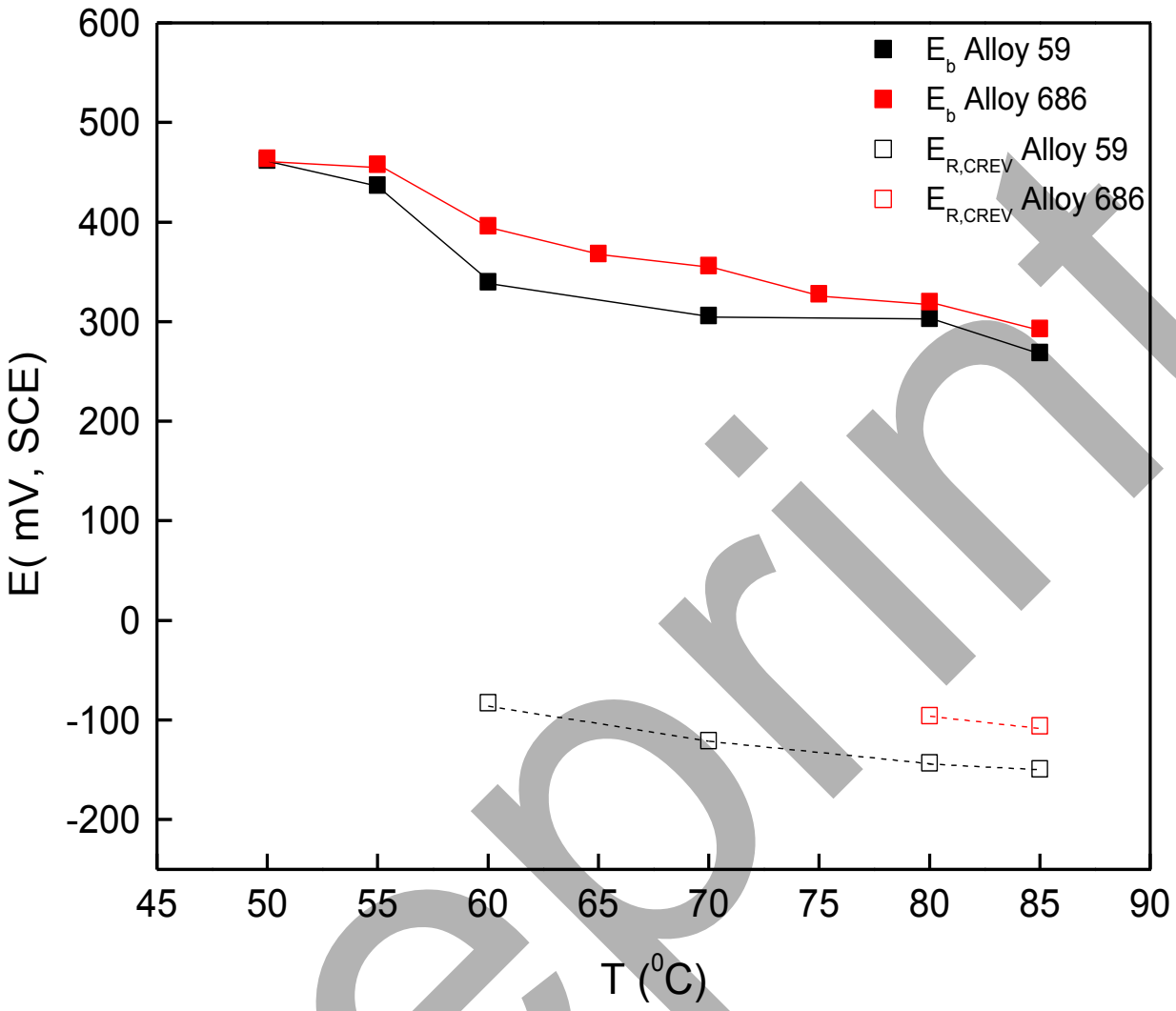

Figure 11. E_b and $E_{R,CREV}$ values recorded using the PD-GS-PD technique on MCA specimens of Alloy 59 and Alloy 686 at different temperatures in 1M NaCl solution.

http://dx.doi.org/10.5006/1170

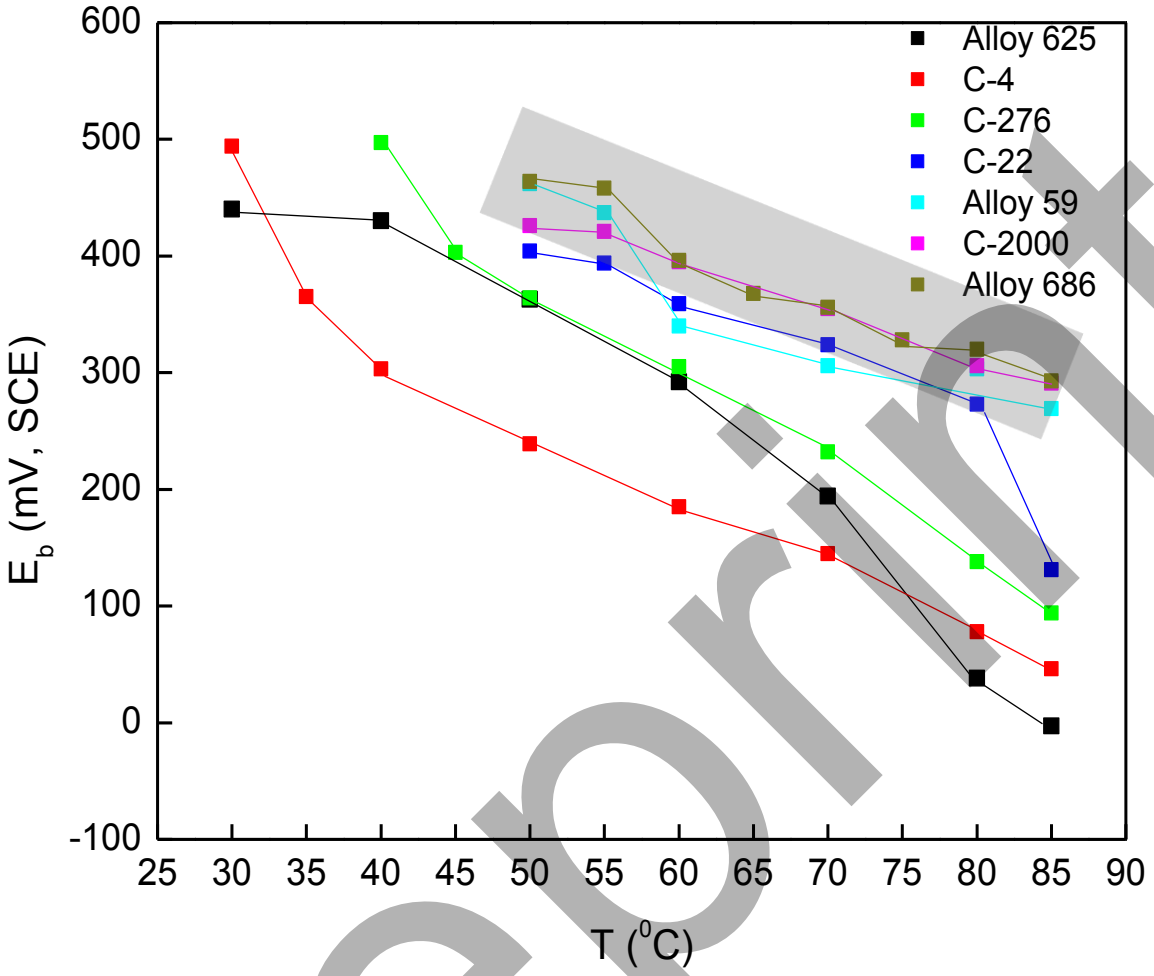

Figure 12. E_b values for various commercial Ni-Cr-Mo (W) alloys as a function of temperature measured in 1M NaCl solution.

http://dx.doi.org/10.5006/1170

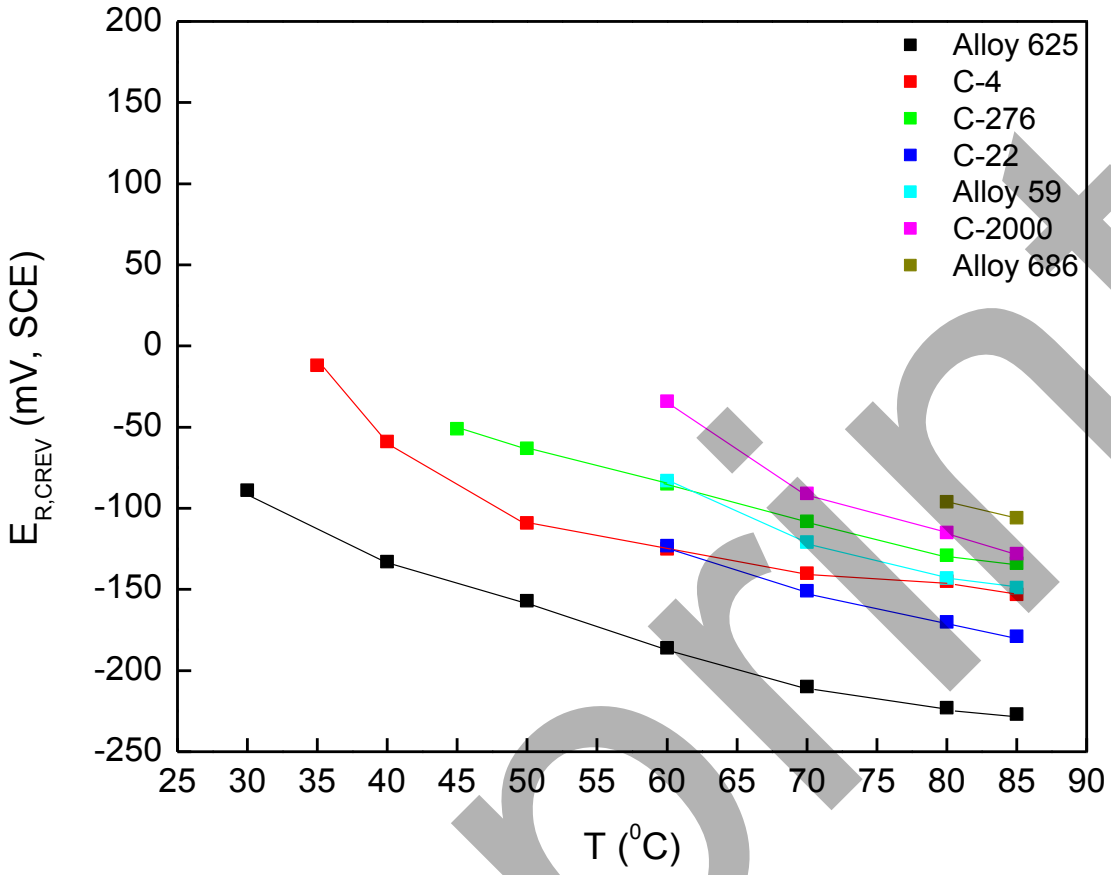

Figure 13. $E_{R,CREV}$ values for various commercial Ni-Cr-Mo (W) alloys as a function of temperature measured in 1M NaCl solution.

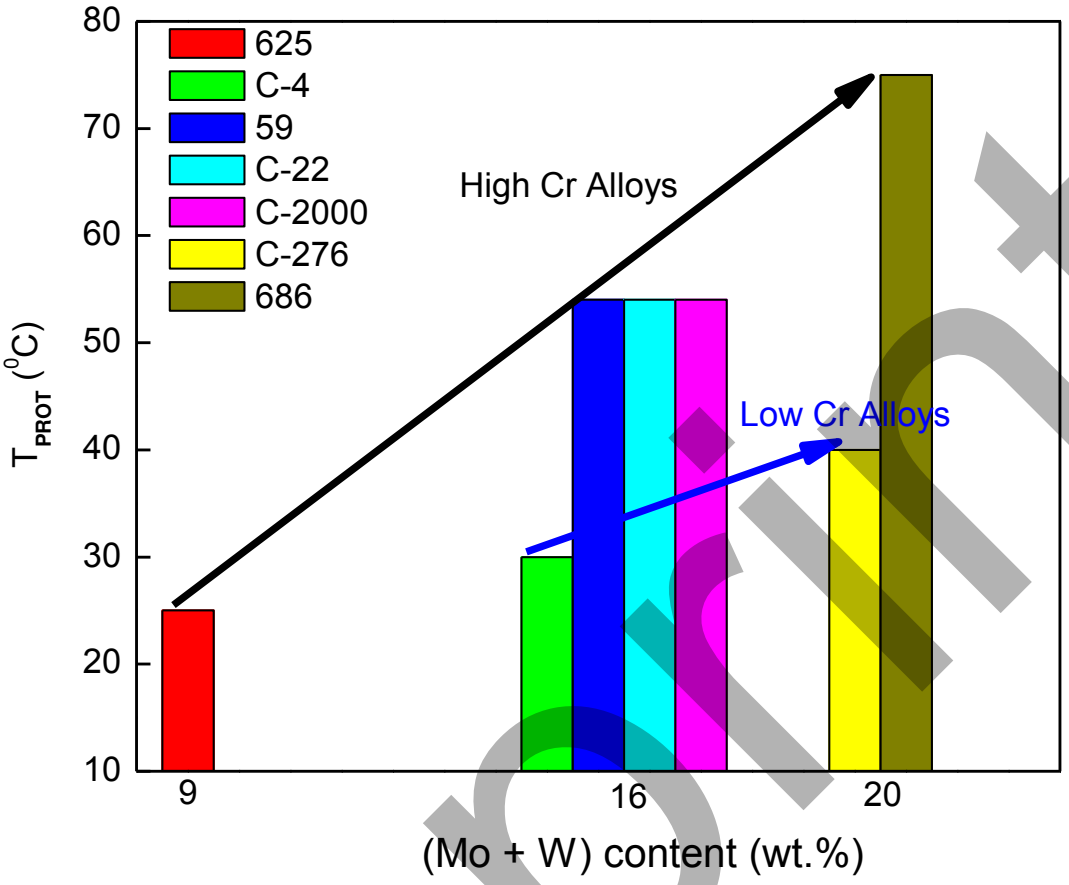

Figure 14. T_{PROT} values as a function of the Mo+W content of a series of commercial Ni-Cr-Mo (W) alloys measured in 1M NaCl solution.

http://dx.doi.org/10.5006/1170

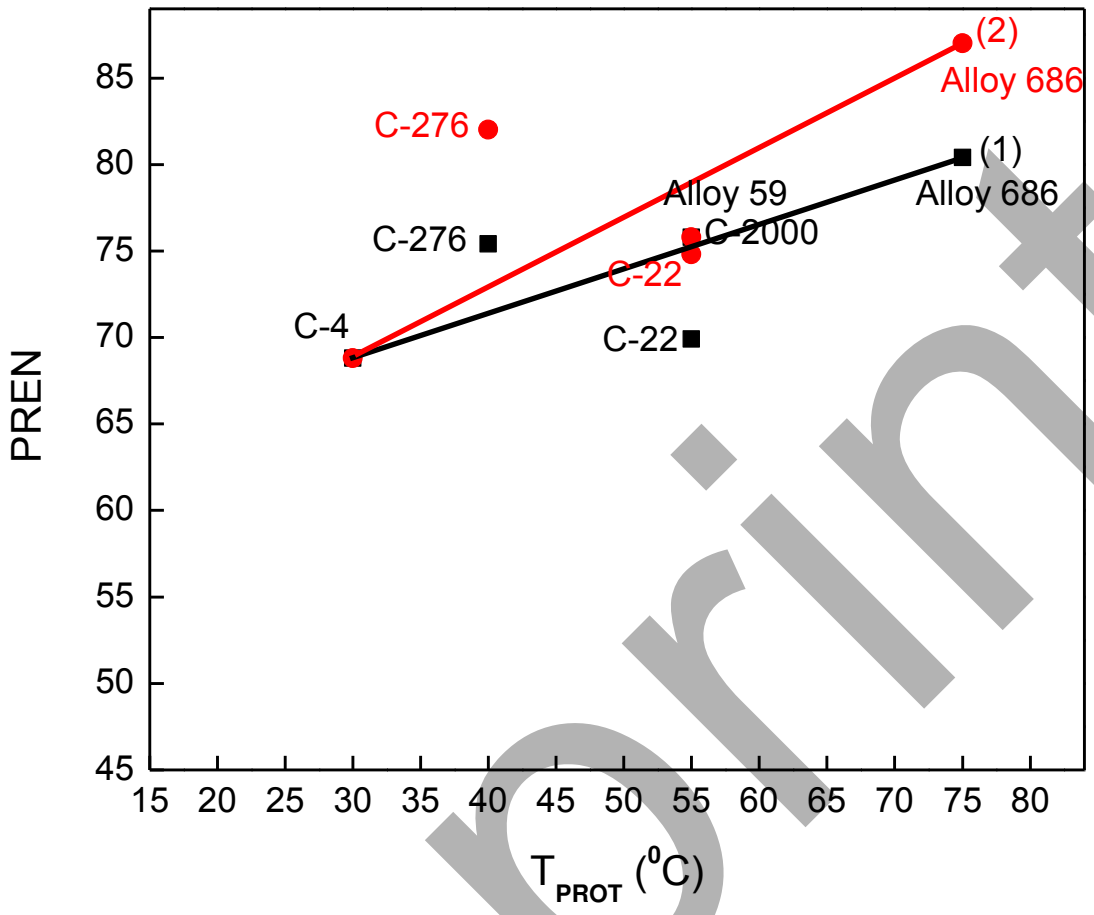

Figure 15. Relationship between T_{PROT} (from Figure 14) and PREN values calculated for various Ni-Cr-Mo (W) alloys: (1) PREN values calculated using relationship (1); (2) PREN values calculated using relationship (2).